OXFORD

Glycan Synthesis

Amyrel, a novel glucose-forming α-amylase from *Drosophila* with 4-α-glucanotransferase activity by disproportionation and hydrolysis of maltooligosaccharides

Georges Feller[2], Magalie Bonneau[3], and Jean-Luc Da Lage[1,3]

[2]Laboratory of Biochemistry, Center for Protein Engineering-InBioS, University of Liège, Liège-Sart Tilman B-4000, Belgium, and [3]UMR 9191 Evolution, Génomes, Comportement et Ecologie, CNRS, IRD, Université Paris-Sud, Université Paris-Saclay, Gif-sur-Yvette F-91198, France

[1]To whom correspondence should be addressed: Tel: +33-1-69-82-37-27; Fax: +33-1-69-82-37-36; e-mail: jean-luc.da-lage@egce.cnrs-gif.fr

Abstract

The α-amylase paralogue Amyrel present in true flies (Diptera Muscomorpha) has been classified as a glycoside hydrolase in CAZy family GH13 on the basis of its primary structure. Here, we report that, in fact, Amyrel is currently unique among animals as it possesses both the hydrolytic α-amylase activity (EC 3.2.1.1) and a 4-α-glucanotransferase (EC 2.4.1.25) transglycosylation activity. Amyrel reacts specifically on α-(1–4) glycosidic bonds of starch and related polymers but produces a complex mixture of maltooligosaccharides, which is in sharp contrast with canonical animal α-amylases. With model maltooligosaccharides G2 (maltose) to G7, the Amyrel reaction starts by a disproportionation leading to G_{n-1} and G_{n+1} products, which by themselves become substrates for new disproportionation cycles. As a result, all detectable odd- and even-numbered maltooligosaccharides, at least up to G12, were observed. However, hydrolysis of these products proceeds simultaneously, as shown by *p*-nitrophenyl-tagged oligosaccharides and microcalorimetry, and upon prolonged reaction, glucose is the major end-product followed by maltose. The main structural determinant of these atypical activities was found to be a Gly-His-Gly-Ala deletion in the so-called flexible loop bordering the active site. Indeed, engineering this deletion in porcine pancreatic and *Drosophila melanogaster* α-amylases results in reaction patterns similar to those of Amyrel. It is proposed that this deletion provides more freedom to the substrate for subsites occupancy and allows a less-constrained action pattern resulting in versatile activities at the active site.

Key words: α-amylase, disproportionation, glycoside hydrolase, 4-α-glucanotransferase, transglycosylation

Introduction

Alpha-amylases (α-1,4-glucan-4-glucanohydrolases) are important digestive enzymes for most living organisms since they carry out the first step in the digestion processes of carbohydrates. Their function is to break down starch and related polysaccharides or oligosaccharides into smaller saccharides down to maltose. It is therefore not surprising that in many animals, plants, fungi or bacteria, the coding genes are duplicated, forming multigene families, whose members are more or less divergent from one another, occasionally originating by horizontal transfer (Da Lage et al. 2002; Da Lage et al. 2007; Da Lage et al. 2013). In true flies (Diptera Muscomorpha), there is a paralogue of the usual α-amylase, named *Amyrel* (standing for *amylase-related*) that was first described in *Drosophila* and only expressed in a part of the larval midgut (Da Lage et al. 1998). *Amyrel* is present in true flies and thus may have originated by duplication more than 100 million years ago (Da Lage et al. 1998; Maczkowiak and Da Lage 2006). However, the function of Amyrel and its biological significance are still unclear. According to its sequence, it has been classified in the glycoside hydrolase family GH13-subfamily 15 in the Carbohydrate Active Enzymes database (www.cazy.org), like other invertebrate α-amylases, as it possesses the conserved sequence regions typical of this family (Stam et al. 2006; Lombard et al. 2014). As in other α-amylases, in all available Amyrel sequences, the residues forming the catalytic triad at the active site are conserved as well as most accessory residues involved in substrate binding and in transition-state stabilization. Three of the four residues that bind the essential calcium ion are conserved, whereas the fourth ligand is the main chain carbonyl of a less-conserved residue. Most Amyrel homologs also display a triad of residues forming a chloride binding site. Accordingly, Amyrel possesses all the recognized signatures of animal α-amylases (D'Amico et al. 2000). However, Amyrel diverges by 40% of the amino acid sequence from the classical α-amylase (Amy), and it has some sequence and structural features that are different from the usual dipteran α-amylases, which may have strong implications on its biochemical properties: an additional fifth disulfide bridge in the domain C, a deletion in the common "flexible loop" that lies close to the catalytic cleft (Ramasubbu et al. 2003; Andre and Tran 2004) and additional specific substitutions that were reported earlier (Maczkowiak and Da Lage 2006).

In a previous study, we have reported the basic enzymological parameters of Amyrel from two *Drosophila* species, *Drosophila melanogaster* and *Drosophila virilis* (Claisse et al. 2016). We have shown that the apparent amylolytic activity of Amyrel was about 30–50 times lower than that of Amy and that the optimal pH was shifted toward mild acidity (pH 6.0 vs. 7.5 for Amy). We also demonstrated that, while *D. melanogaster* Amyrel was chloride-activated, like most animal α-amylases (D'Amico et al. 2000), Amyrel from *D. virilis*, having a glutamine (Q323) instead of the conserved arginine (R323) at the chloride-binding site, was independent of chloride. Moreover, this latter enzyme, engineered with an arginine instead (Q323R), displayed an enhanced amylolytic activity.

In the present study, we report that Amyrel has a much more complex activity pattern than previously thought and is currently unique in animals. Indeed, Amyrel displays both hydrolytic α-amylase activity and a 4-α-glucanotransferase transglycosylation activity. We show that Amyrel is able to process maltotriose and even maltose, unlike Amy, and that the final end-product is glucose followed by maltose, with a transient reaction phase where long maltooligosaccharides are formed. We also show that the deletion within the flexible loop is a main structural determinant of the unusual Amyrel activity.

Results

Amyrel is a glucose- and maltooligosaccharide-forming α-amylase

Animal α-amylases are endo-acting enzymes that hydrolyze starch and related polysaccharides into maltose (G2) and maltotriose (G3) as major end-products, as shown in Figure 1A and B for porcine pancreatic α-amylase and *D. melanogaster* Amy α-amylase. Few longer oligosaccharides appear in the soluble starch digest. This has been related to their processivity, i.e. the enzyme can remain bound on its substrate, then slides along the polysaccharide chain and performs the so-called multiple attack (Mazur and Nakatani 1993; Bijttebier et al. 2008). In sharp contrast, the initial products of Amyrel reaction on soluble starch were all odd- and even-numbered oligosaccharides detectable by thin layer chromatography (TLC), including glucose (Figure 1C). Upon prolonged incubation, glucose was the major end-product followed by maltose, which is similar to a α-glucosidase-like activity.

Amyrel reacts specifically with α-(1–4) glycosidic bonds as starch, glycogen, amylose and amylopectin digests produced the same pattern (with G1, G2 and G_n accumulation), whereas oligosaccharides containing α-(1–6) bonds (isomaltotriose, pullulan and dextran), α-(1–3) bonds (nigeran) or β-(1–4) bonds (cello-oligosaccharides) remained unreacted. No amylosucrase activity was detected, nor activity on glucose, saccharose, trehalose and raffinose. No reaction of Amyrel on α-cyclodextrin (cyclic G6) and β-cyclodextrin (cyclic G7) was detected but, very interestingly, γ-cyclodextrin (cyclic G8) digests displayed a TLC pattern with G1–G8 accumulation and trace amounts of products higher than G8 (Supplementary Figure S1). This suggests that the first step in the γ-cyclodextrin reaction is hydrolysis, which opens the cyclic structure. Oligosaccharides with a degree of polymerization (DP) higher than G8 are not hydrolytic products; therefore, they are attributed to a transglycosylase activity. By contrast, the Amy α-amylase only produced low amounts of G2 and G3 upon prolonged incubation with γ-cyclodextrin.

Disproportionation of maltooligosaccharides

The appearance of multiple maltooligosaccharides in the initial phase of starch and γ-cyclodextrin hydrolysis by Amyrel suggests a distinct mode of action as compared to canonical animal α-amylases. This was further analyzed by comparing the reaction time course with oligosaccharides G2–G7 as substrates between Amy and Amyrel (Figure 2A). Remarkably, although G2 reacted very slowly, all odd- and even-numbered oligosaccharides detectable by TLC were observed in the reaction mixture of Amyrel for G2–G7 (Figure 2A and B, Supplementary Figure S2), revealing a remarkable transglycosylation activity and more precisely a 4-α-glucanotransferase (4-α-GTase) activity. The synthesized bonds have to be α-(1–4) glycosidic bonds because, upon prolonged incubation, all transglycosylation products were eventually hydrolyzed into glucose and maltose, whereas Amyrel is inactive on other glycosidic bonds (as mentioned in the previous paragraph). The size of the transglycosylation products was $\geq$G12 in TLC (Figure 2B), whereas MALDI-TOF mass spectrometry unambiguously detected up to G10 as Na+ adducts (Supplementary Figure S3), like most oligosaccharides in such experiments (Clowers et al. 2008). Mass
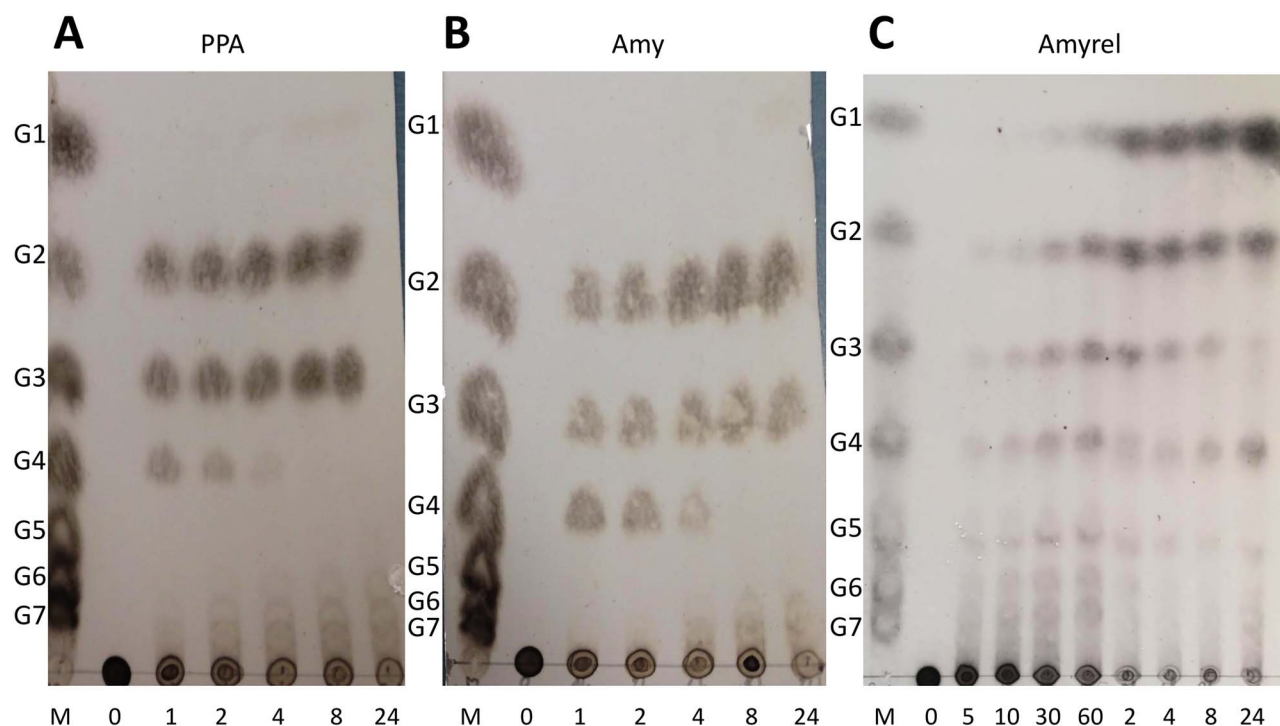
Fig. 1. TLC of reaction time courses of soluble starch (5 mg/mL) digested by (**A**) PPA, (**B**) Amy α-amylase from *D. melanogaster* and (**C**) Amyrel from *D. melanogaster*. Final concentration of enzymes: 15 nM PPA, 6 nM Amy, 150 nM Amyrel. M, maltooligosaccharide ladder. Reaction times are indicated in hours (**A**, **B**) and in minutes and hours (**C**).

spectrometry also confirmed that the products were genuine, unmodified maltooligosaccharides (mass difference of 162 between species) which also migrated concurrently in TLC with commercially available G1–G7. Accordingly, the reaction products of Amyrel were used as convenient and inexpensive TLC markers.

In order to characterize the reaction mechanism, the first products of Amyrel were identified by TLC at low enzyme concentrations. For all oligosaccharide substrates from G2 to G7, the first products were invariably G_{n-1} and G_{n+1} (Figure 3, Supplementary Figure S4). This indicates that transglycosylation by Amyrel proceeds via a disproportionation reaction according to the general pathway:

$$2\ G_n \rightarrow G_{n-1} + G_{n+1}.$$
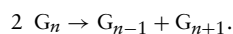
This reaction implies the exo-cleavage of G1 from one end of the first G_n substrate (providing G_{n-1}), the formation of a glucosyl-enzyme intermediate EG1 and the transfer of G1 to an end of the second G_n acceptor (providing G_{n+1}). Following this initial step, the fast appearance of maltooligosaccharides shorter than G_{n-1} and longer than G_{n+1} demonstrated that the first products by themselves became substrates for new rounds of disproportionation.

Subsite requirements and glycosidic acceptors

Maltose (G2) is the shortest oligosaccharide processed by Amyrel (Supplementary Figures S2 and S4), whereas canonical animal α-amylases are inactive on this substrate. This indicates that occupancy of only two subsites (−1 and +1 with respect to the cleavage site) in the Amyrel active site is sufficient to initiate the reaction with formation of a glucosyl-enzyme intermediate EG1 followed by disproportionation of G2 into G1 + G3. To evaluate

the relative activity of Amyrel on maltooligosaccharides, the time of appearance of the first products on TLC was recorded and normalized for protein concentration (Table I). It can be seen that the relative activity sharply increases with the length of the oligosaccharides up to G6 and G7. This shows that optimal subsite occupancy strongly stimulates Amyrel disproportionation activity. It should be noted that G3 hydrolysis into G2 and G1 has been reported for porcine pancreatic α-amylase (PPA) (Robyt and French 1970). However, for the latter, this is a minor activity requiring high substrate concentration and 1000 times more enzyme to achieve hydrolysis and, as a result, this activity is not observable under standard conditions of hydrolysis of polysaccharides by anima l α-amylases (Figures 1 and 2). Accordingly, Amyrel remarkably differs from animal α-amylases by its ability to disproportionate maltose and by its strongly enhanced activity on maltotriose.

Addition of *p*-nitrophenyl moiety (*p*NP)-tagged oligosaccharides in the Amyrel reaction medium also helped to decipher its reaction mechanism. When *p*NP was added to a substrate such as G3, no intermediate bands typical of *p*NP-tagged oligosaccharides were observed. This reveals the inability of *p*NP alone to participate to the transglycosylation reaction. Furthermore, the chromogenic substrate G1–*p*NP was not hydrolyzed by Amyrel since no product was detected in TLC nor was *p*-nitrophenolate anion released since the absorbance A_{405} of the reaction medium was unchanged (Supplementary Figure S5). This shows that the *p*NP cannot mimic a glucopyranose unit for subsite occupancy.

By contrast, the substrate G2–*p*NP was processed by Amyrel: In a first step, G2–*p*NP underwent a disproportionation reaction leading to products G1–*p*NP, which accumulated, and G3–*p*NP (Supplementary Figure S6). Such reaction involving the nonreducing end of both products (as the reducing end is blocked by the *p*NP
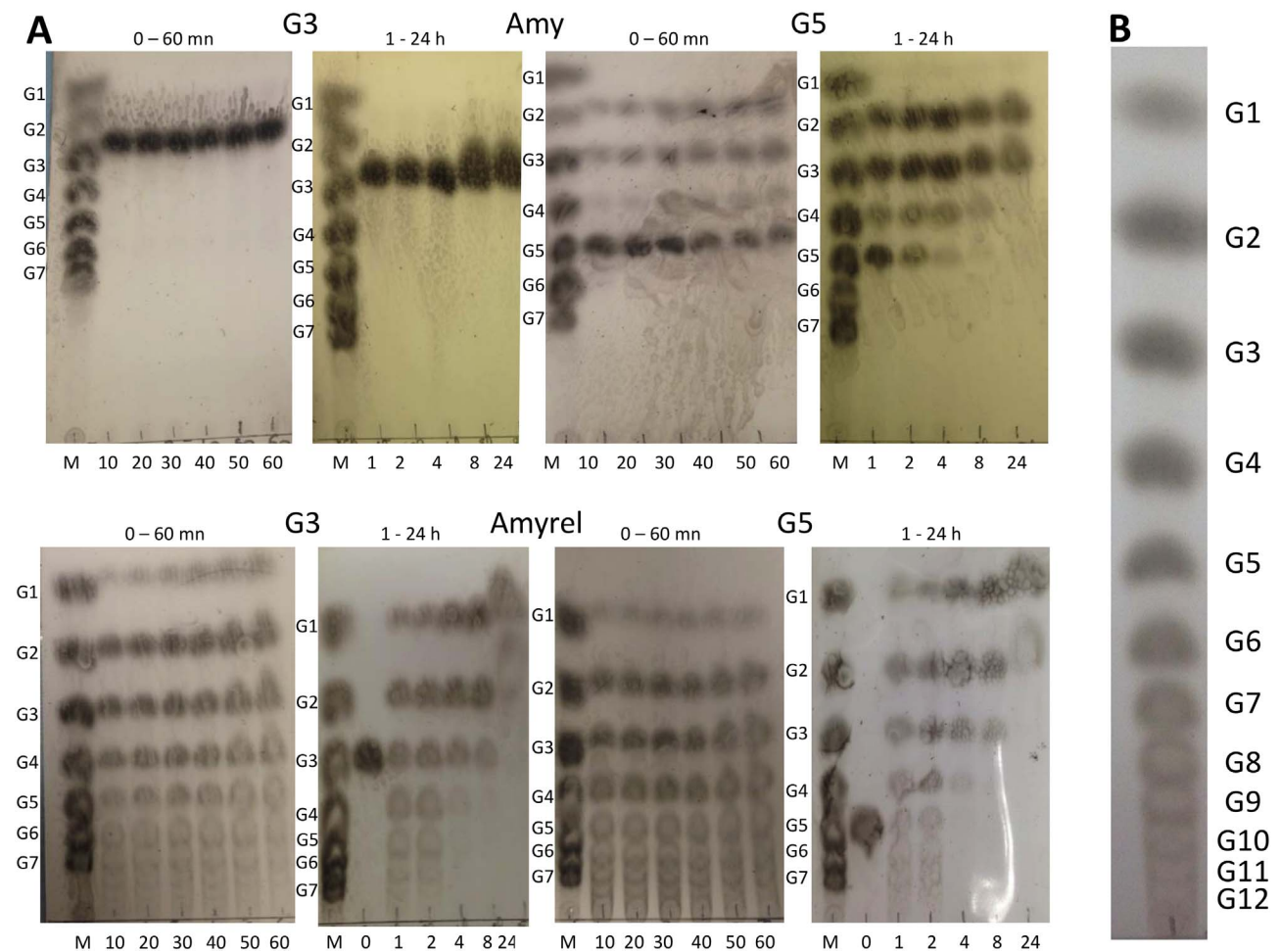
Fig. 2. (**A**) TLC of reaction time courses of maltooligosaccharides G3 and G5 (5 mg/mL) digested by the Amy α-amylase (upper panel) and Amyrel (lower panel) from *D. melanogaster*. Final concentration of enzymes: 6 nM Amy, 150 nM Amyrel. M, maltooligosaccharide ladder. Reaction times are indicated in minutes and hours. (**B**) Typical TLC pattern of maltooligosaccharides produced by Amyrel (450 nM) with G3 (20 mg/mL) as substrate after 30-min incubation. Maltooligosaccharides are numbered up to the last detectable product.

Table I. Disproportionation activity of Amyrel on maltooligosaccharides estimated by the time of appearance in seconds, normalized for protein concentration (s/µg), of the first products G_{n-1} and G_{n+1} on TLC, and relative disproportionation activity with respect to G7 as the fastest reacted substrate

| Substrate	G2	G3	G4	G5	G6	G7
s/µg	3400	57	14	6	5	4
Activity (%)	0.1	7	27	68	86	100

group) implies that G2–*p*NP binds to subsites -1, $+1$ (and possibly $+2$ occupied by the *p*NP group) with respect to the cleavage site (Figure 4). In the next step, the G3–*p*NP product formed was disproportionated into low amounts of higher DP products, but no larger than G6–*p*NP. However, *p*-nitrophenol was simultaneously released in the reaction mixture, as shown by the increase of A_{405} (Supplementary Figure S5). Accordingly, G2–*p*NP can also bind to subsites -2, -1 and $+1$, the latter being occupied by the *p*NP group (Figure 4), with release of G2 and *p*NP. At this stage, G2 should become the substrate for disproportionation toward longer oligosaccharides up to G6, as observed by TLC. In addition, hydrolysis of the terminal *p*NP group from G*x*–*p*NP should contribute to both the increase of A_{405} and to the appearance of maltooligosaccharides,

limited to G6 in our conditions. The low DP of the disproportionation products could be attributed to the very slow disproportionation of G2 (Table I) before the final hydrolysis of the products into G1–*p*NP, G1 and G2. Finally, it is also worth mentioning that the reaction pattern of G2–*p*NP demonstrates that both disproportionation and hydrolysis reactions occur concomitantly.

Interestingly, when G3 or G5 substrates were mixed in equimolar amounts with the inert G1–*p*NP, the absorbance at 405 nm of the reaction medium increased (Supplementary Figure S5). TLC analysis of the reaction medium (Supplementary Figure S7) revealed, in addition to the usual G_x disproportionation products, the synthesis of G2–*p*NP, which is prone to hydrolysis with *p*NP release (as shown in the previous paragraph). The synthesis of G2–*p*NP demonstrates
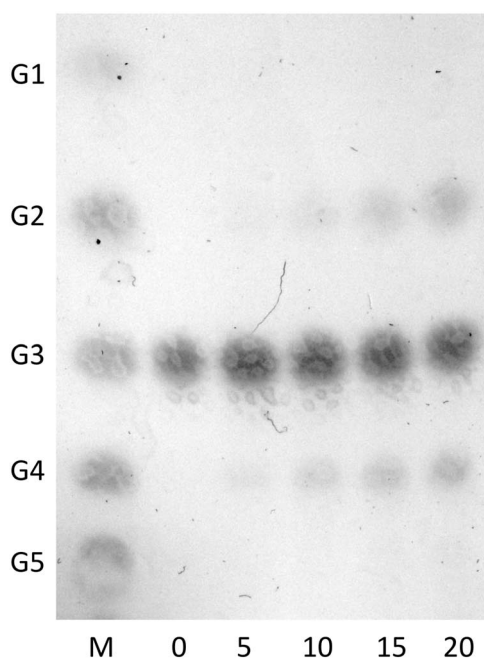
Fig. 3. Disproportionation of maltooligosaccharides by Amyrel. TLC of the reaction time course by Amyrel (35 nM) with G3 (5 mM) as substrate showing the appearance of the first products G_{n-1} and G_{n+1}. M, maltooligosaccharide ladder. Reaction times are indicated in minutes.
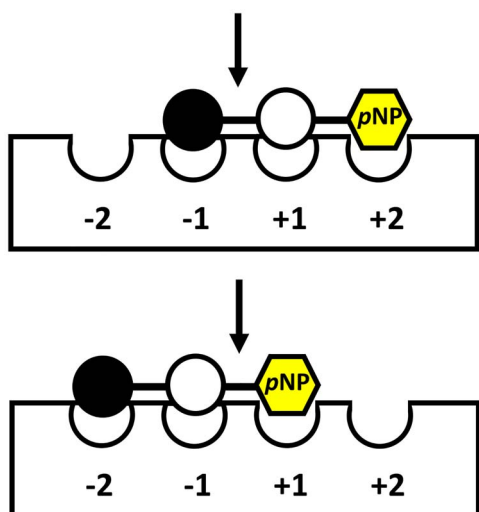
Fig. 4. Binding of G2–pNP in the Amyrel active site. Subsites are numbered with respect to the cleavage site (arrow). Closed circle, nonreducing end of the substrate; open circle, glucopyranose unit. Upper panel: binding mode resulting in G1 + G1–pNP release. Lower panel: binding mode resulting in G2 + pNP release. Only subsites required for G2–pNP binding are depicted.

that G1–pNP can be the acceptor of the glucosyl-enzyme intermediate EG1 during the disproportionation reaction, and therefore, also suggests that glucose could be an acceptor. In order to detect if the exogenous free glucose could participate to the disproportionation reaction, trace amount of ^{14}C-glucose were added to the Amyrel reaction medium using G3 or G4 as substrates. After TLC analysis, the autoradiograms revealed that all products formed were ^{14}C-labeled (Supplementary Figure S8) and accordingly confirmed that G1 alone is an acceptor.

The proposed disproportionation reaction was also probed by comparing the reaction pattern of Amyrel on G7–pNP and on Et–G7–pNP in which the ethylidene group Et blocks the nonreducing end. The substrate G7–pNP provided a complex pattern of G_n and G_n–pNP with high DP products (Supplementary Figure S9A). By contrast, the concentration of high DP products was significantly lower with Et–G7–pNP (Supplementary Figure S9B). This strongly suggests that Et-blocked oligosaccharides cannot be acceptors during disproportionation and, accordingly, that a free nonreducing end is required. This also implies that high DP products arise from the internal hydrolysis of Et–G7–pNP with further disproportionation of the released unmodified and pNP-tagged oligosaccharides. Furthermore, Et-glucose was not released from Et–G7–pNP during the reaction, even under prolonged incubation (Supplementary Figure S9C), showing that a glucosyl-enzyme intermediate E-Et-G1 was not formed. The lack of Et–G1 indicates that the Amyrel subsite −1 displays a strict specificity for an unmodified glucopyranose unit.

Balance between hydrolysis and transglycosylation

Following extended incubation, all Amyrel reaction products are eventually hydrolyzed into glucose and maltose (Figure 2A). This indicates that in the reaction time course, the equilibrium between hydrolysis and transglycosylation is only slightly in favor of hydrolysis, which is in sharp contrast with animal α-amylases for which hydrolysis is strongly favored, without the appearance of detectable transglycosylation products as shown in Figures 1 and 2A. In order to check this aspect and due to the complexity of the products formed by Amyrel, the reaction was monitored by isothermal titration calorimetry. In this approach, the enzyme is injected into the microcalorimeter cell containing the substrate, and the heat release of α-(1–4) glycosidic bond hydrolysis is recorded (D'Amico et al. 2006). In the following experiments, it was assumed that α-(1–4) glycosidic bond synthesis occurs with heat absorption unlike hydrolysis which is exothermic.

When the α-amylase Amy was injected into its substrates, hydrolysis proceeded immediately with net heat release (Figure 5, Supplementary Figure S10), allowing the determination of the catalytic rate constant k_{cat} (Table II). The activity remained at a steady state (V_{max} under saturating substrate concentration), then decreased as a result of substrate depletion according to a Michaelis–Menten mechanism. In sharp contrast, injection of Amyrel into starch, G3 (Figure 5) and G4 (Supplementary Figure S10) did not achieve steady state as the activity slowly increased with time. This behavior indicates that, during the recording, a reaction competes with hydrolysis, which can be attributed to α-(1–4) glycosidic bond synthesis. These profiles also show that the hydrolysis rate exceeds the synthesis rate, as already observed in TLC. With Amyrel injection into G5, G6 and G7, a moderate initial hydrolysis was recorded (Table II, Supplementary Figure S10). Such hydrolysis should occur on the internal α-(1–4) bonds of the substrate and not by hydrolysis of the covalent glucosyl-enzyme intermediate EG1 because glucose does not appear in the early products.

It has been reported that the 4-α-GTase activity can be inhibited by glucose (Kaila and Guptasarma 2019). This aspect was checked for Amyrel using G5 as substrate and increasing concentrations of added glucose (Supplementary Figure S11). It can be seen that Amyrel was inhibited by high glucose concentrations as products with DP higher than the substrate decreased in abundance and became close to the detection limit. Such inhibition by glucose, which is the main end-product of Amyrel, should contribute to slow down significantly its 4-α-GTase activity during the reaction time course.
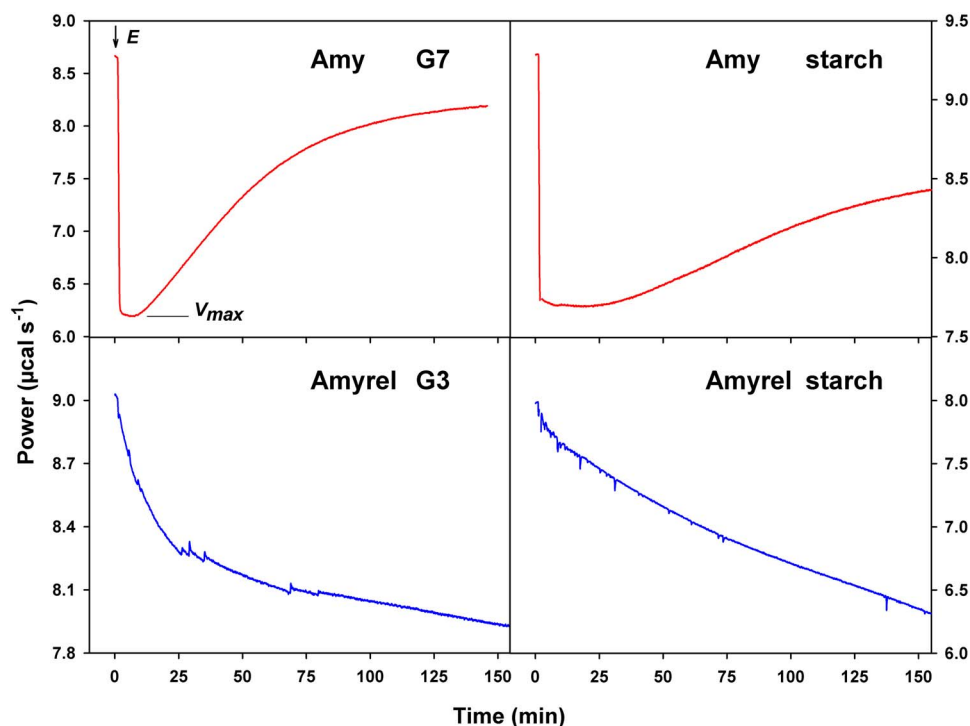
Fig. 5. Reaction time courses of Amy and Amyrel on polysaccharides recorded by ITC. The records start with the injection (arrow) of enzyme (E) in the reaction vessel. For Amy, the heat release of α-(1–4) hydrolysis reaches a steady state (V_{max}) allowing the k_{cat} determination. For Amyrel, a steady state is not reached, indicating a competing reaction with opposite enthalpy, attributed to α-(1–4) bond synthesis.

Table II. Catalytic rate constants k_{cat} of the α-amylase Amy, of Amyrel and of the mutant Amy ΔGHGA, expressed as the number of glycosidic bonds hydrolyzed per active site and per second, recorded by isothermal titration calorimetry

|	k_{cat} (s^{-1})					
	Starch	G3	G4	G5	G6	G7
Amy[a]	306	nd	13	159	268	245
Amyrel	H/T	H/T	H/T	11	12	13
Amy ΔGHGA	H/T	nd	H/T	9	13	11

nd, not detected; H/T, simultaneous hydrolysis and transglycosylation. [a]Data from (Commin et al. 2013).

A structural determinant of transglycosylation

At the structure and sequence level, one major difference between Amyrel and most animal α-amylases is a Gly-His-Gly-Ala deletion within the so-called flexible loop, which undergoes a large displacement upon substrate processing in animal-type α-amylases (Qian et al. 1994). In order to evaluate the possible effects of this deletion, the corresponding Gly-His-Gly-Ala residues were deleted in the α-amylase Amy from *D. melanogaster* and in PPA, resulting in mutant enzymes Amy ΔGHGA and PPA ΔGHGA, respectively. Activity measurements by the Bernfeld method using starch as a substrate showed that the apparent k_{cat} (apparent as hydrolysis and disproportionation proceed simultaneously) of the purified mutants were drastically reduced at values similar to that of Amyrel (Table III). More significantly, however, TLC revealed that both mutants were able to disproportionate short oligosaccharides and provide reaction patterns similar to that of Amyrel (Figure 6), which is in sharp contrast with the parent α-amylases. In addition, the mutant Amy ΔGHGA was able to slowly disproportionate maltotriose, although this

property was not observed in PPA ΔGHGA (Figure 6). Furthermore, when analyzed by ITC, Amy ΔGHGA displayed reaction profiles that were closely related to those of Amyrel (Supplementary Figure S10), with competing hydrolysis and synthesis of α-(1–4) glycosidic bonds from starch and G4 as well as an initial weak hydrolysis of G5, G6 and G7 (Table II). Moreover, the optimum pH for activity of Amy ΔGHGA was shifted from pH 7.5 in Amy to more acidic values (Supplementary Figure S12), which was similar to the optimum pH of Amyrel (Claisse et al. 2016). These results highlight the essential involvement of the deletion ΔGHGA within the flexible loop in the unusual reaction pattern of Amyrel.

Nevertheless, some discrepancies were observed between both mutants and Amyrel. Although the ΔGHGA deletion provided a glucose-forming activity in both mutants, G1 was not the major end-product, which is in contrast with Amyrel, and the mutants retained the final digestion profile of the parent enzymes with G2 and G3 as main end-products. Moreover, Amy ΔGHGA was unable to incorporate exogenous ^{14}C-glucose in the disproportionation products (not
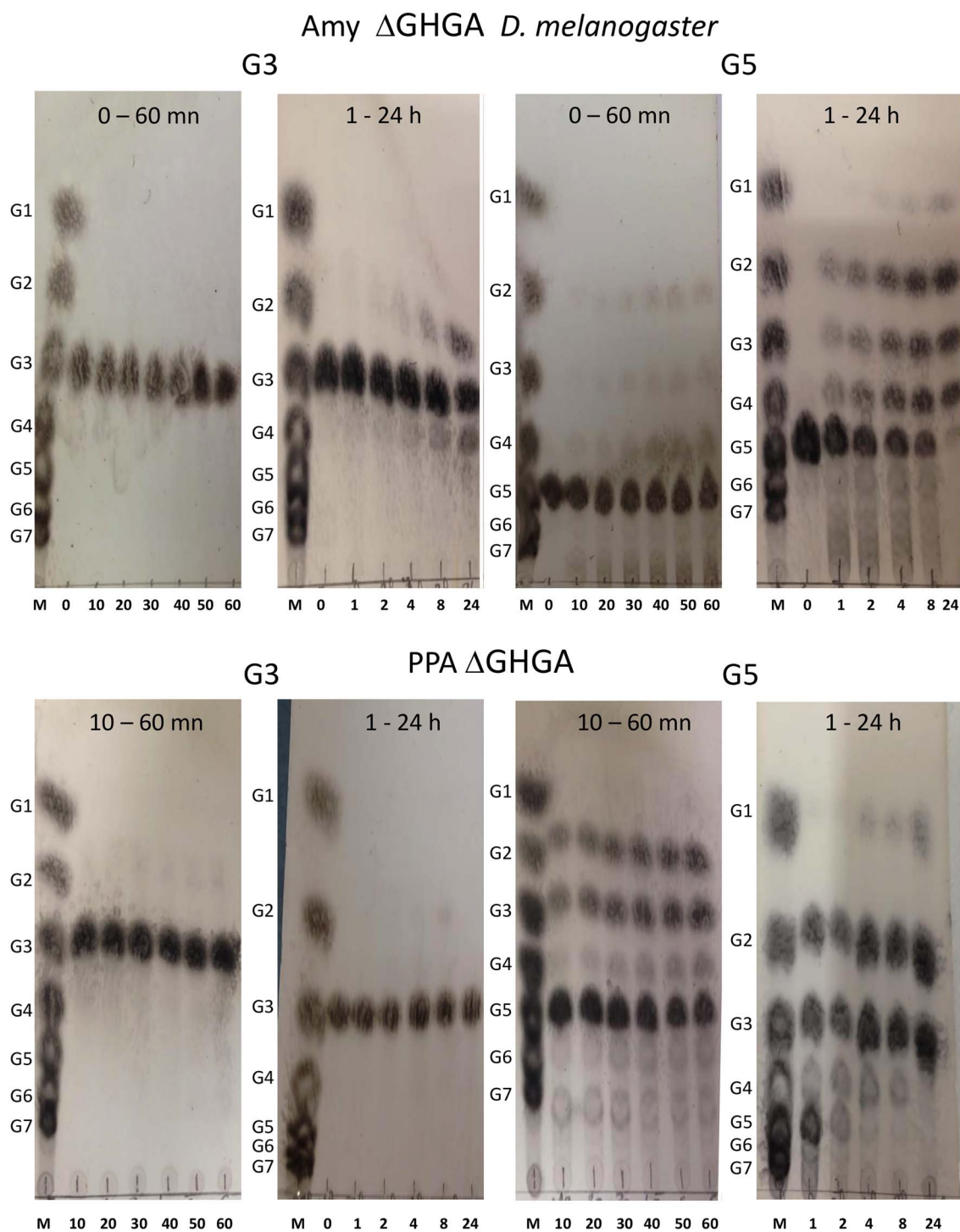
Fig. 6. TLC of reaction time courses of maltooligosaccharides G3 and G5 (5 mg/mL) digested by the mutants Amy $\triangle$GHGA (upper panel, 20 nM) and PPA $\triangle$GHGA (lower panel, 140 nM). Note the disproportionation of G3 by Amy $\triangle$GHGA as well as the appearance of G1 and of multiple maltooligosaccharides with G5 as substrate for both mutants. M, maltooligosaccharide ladder. Reaction times are indicated in minutes and hours.

shown). These discrepancies suggest that, beside the $\triangle$GHGA deletion, additional residues should be involved in the specific reaction profile of Amyrel.

In this respect, a substitution in the Amyrel primary structure attracted our attention. It has been reported that the mutation Tyr151Met introduced in the subsite +2 of human salivary α-amylase provided a limited transglycosylation activity (Remenyik et al. 2003). This Tyr151 residue is conserved in animal α-amylases, with only some rare exceptions. By contrast, in all Amyrel homologs, this position is occupied by a Trp residue. Accordingly, the corresponding

Table III. Activity on 1% soluble starch of Amyrel, the α-amylases Amy and PPA and of the deletion mutants (mean $\pm$ S.E.M., $n = 3$) measured by the dinitrosalicylic acid method (Bernfeld 1955)

	Apparent k_{cat} (s^{-1})
Amyrel[a]	12.9 ± 0.5
Amy	586 ± 18
Amy ΔGHGA	42.7 ± 0.6
PPA	402 ± 13
PPA ΔGHGA	15.3 ± 0.6

S.E.M., standard error of the mean. [a]Data from (Claisse et al. 2016).

position has been mutated into Trp142Tyr in Amyrel, and the reverse mutation Tyr140Trp has been introduced in the α-amylase Amy from *D. melanogaster*. The amylolytic activities of Amyrel Trp142Tyr and its wild-type counterpart were similar. By contrast, the Amy Tyr140Trp mutant had a 6-fold decrease of activity compared to the wild-type. The reaction patterns of Amyrel Trp142Tyr on maltooligosaccharides did not display detectable differences with the wild-type enzyme (not shown). In sharp contrast, the mutant Amy Tyr140Trp acquired a significant glucose-forming activity on starch, G3 and G5 (Supplementary Figure S13) and furthermore it was able to hydrolyze G3, whereas the wild-type Amy is devoid of such activity (Figure 2). This mutation provides a α-glucosidase-like activity to Amy and shows that Trp142 in Amyrel likely contributes to its atypical reaction pattern.

Discussion

Several maltooligosaccharide-forming α-amylases from bacteria and some fungi have been described (Pan et al. 2017). Among them, a few enzymes produce glucose in addition to higher DP products, and in rare cases, limited transglycosylation activity has been reported (Xu et al. 2018). In this respect, Amyrel is unique to date as it is an animal α-amylase, glucose is the major end-product with maltose and it displays a remarkable transglycosylase activity (Figure 2). Surprisingly, the reaction pattern of Amyrel in TLC (Figures 1 and 2) is strikingly similar to those reported for 4-α-GTases from hyperthermophilic archaea such as *Thermococcus onnurineus* (Kaila and Guptasarma 2019) or *Pyrococcus furiosus* (Kaila et al. 2019). However, these enzymes are totally unrelated to Amyrel at the primary, tertiary and quaternary structures. These glycoside hydrolases found in Archaea belong to the GH57 family according to the CAZy classification (Lombard et al. 2014), whereas Amyrel belongs to the GH13 family, they are folded in a $(\beta/\alpha)_7$ barrel, whereas Amyrel has a predicted $(\beta/\alpha)_8$-fold and are homo-dimeric, whereas Amyrel is monomeric. Closely related reaction patterns were also reported for GH77 4-α-GTases, including the plant D-enzyme and microbial amylomaltases (Takaha and Smith 1999; Ahmad et al. 2015). Within GH13 members, microbial CGTases (EC 2.4.1.19) also produce multiple maltooligosaccharides in addition to cyclodextrins, although maltose is not reacted, with the only exception of *B. megaterium* CGTase (Ahmad et al. 2015). In Eukaryotes, only the glycogen debranching enzyme has been reported to have a 4-α-GTase activity, which transfers a maltotriosyl group from a glycogen branch point to a neighboring nonreducing end. This large GH13 enzyme (170 kDa) is bifunctional and possesses an additional α-1,6 glucosidase active site (Zhai et al. 2016). It follows that Amyrel is currently unique in animals as it possesses both α-amylase (EC 3.2.1.1) and 4-α-glucanotransferase (EC 2.4.1.25) activities.
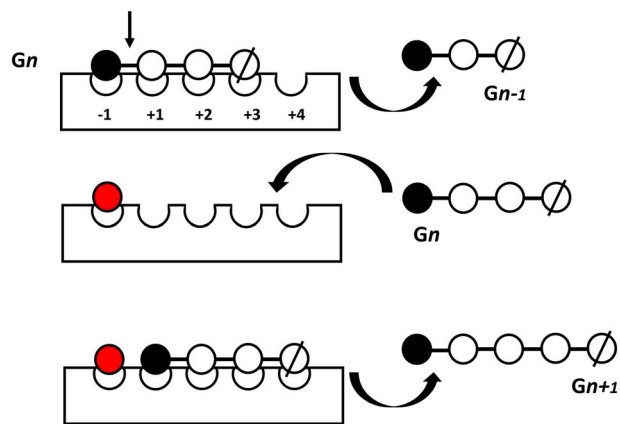
Fig. 7. Disproportionation reaction of maltooligosaccharides by Amyrel, illustrated for G4. Subsites are numbered with respect to the cleavage site (arrow). Closed circle, nonreducing end; open circle, glucopyranose unit; open slashed circle, reducing end; in red, the covalent glucosyl-enzyme intermediate. For details, see text. Only subsites required for G4 binding are depicted.

With short oligosaccharides G2–G7, an initial disproportionation reaction has been clearly evidenced (Figure 3). This disproportionation reaction requires the formation of the enzyme–substrate complex EG1 and exo-cleavage of the substrate by the catalytic nucleophile Asp188 (Amyrel numbering, by homology) and the general acid/base catalyst Glu225, with G_{n-1} as the leaving group. This exo-cleavage occurs at the nonreducing end of G_n because, in the case of exo-cleavage at the reducing end, glucose would be the first product as the leaving group and G_{n+1} would not be synthesized. The reaction pattern of the nonreducing end blocked Et–G7–pNP (Supplementary Figure S9) also supports such cleavage. According to the double displacement mechanism of α-amylases retaining the anomeric configuration (Uitdehaag et al. 1999) and performing transient transglycosylation (Qian et al. 1994; Aghajari et al. 2002), the covalent glucosyl-enzyme intermediate EG1 should be formed by Amyrel Asp188 and the glucosyl residue (glycosylation step). In the next nucleophilic displacement step, the incoming substrate G_n becomes the transglycosylation acceptor of G1 at its nonreducing end (deglycosylation step), leading to the release of G_{n+1} product, as summarized below and as illustrated in Figure 7.

$$E + G_n \rightleftharpoons EG_n \rightleftharpoons EG1 + G_{n-1} \rightleftharpoons EG1 + G_n \rightleftharpoons EG1G_n \rightleftharpoons E + G_{n+1}.$$
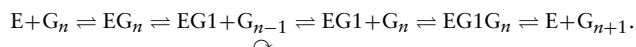
In this pathway, both products can be either hydrolyzed into shorted oligosaccharides or become substrates for a new round of disproportionation, which results in the production of odd- and even-numbered maltooligosaccharides. A similar disproportionation mechanism has been proposed for the bacterial amylosucrase from *Neisseria polysaccharea* belonging to GH13 (Albenne et al. 2002), with however noticeable differences. Amylosucrase mainly produces G_{n-1} and G_{n+1} and minor amounts of G_{n-2} and G_{n+2}, in contrast with the multiple DP of oligosaccharides synthesized by Amyrel. In contrast to Amyrel, amylosucrase is unable to release pNP from G_n–pNP tagged at the reducing end. Lastly, amylosucrase does not hydrolyze its transglycosylation products, which is in sharp contrast to Amyrel which gives G1 and G2 as the final reaction products. The disproportionation mechanism has been described for

many glycoside hydrolases, such as the plant D-enzyme or microbial amylomaltases, CGTases and 4-α-GTases but not in animals, with the noticeable exception of Amyrel.

A distinctive feature of Amyrel resides in its glucose-forming activity. In our conditions, glucose never appeared before maltose, and therefore, maltose disproportion into G1 and G3 appears as a primary source of glucose build-up. However, during the disproportionation reaction, water could become a competitive nucleophile of glycosidic acceptors in the deglycosylation step (Abdul Manas et al. 2018), leading to the hydrolysis of the glucosyl-enzyme intermediate EG1 and to glucose release. This is demonstrated by the final accumulation of glucose, with lower amounts of maltose and no residual G3 upon extended reaction. Furthermore, glucose inhibits the 4-α-GTase activity of Amyrel (Supplementary Figure S11) and should therefore contribute to favor the final hydrolysis of the products in the reaction medium. It is also worth mentioning that glucose alone can be the transglycosylation acceptor of EG1 as ^{14}C-glucose was incorporated in all Amyrel products (Supplementary Figure S8). Microcalorimetric measurements have shown that hydrolysis and synthesis of α-(1–4) glycosidic bonds by Amyrel proceeded simultaneously, with a slightly favored hydrolytic activity. In this respect, a true transglycosylation activity by Amyrel cannot be ruled out: In the initial glycosylation step, a glycosyl-enzyme intermediate EG_x could be formed, but instead of being hydrolyzed, the G_x moiety could be transferred to another oligosaccharide acceptor. However, as a result of the complex reaction pattern of Amyrel, such transglycosylation activity has not been unambiguously probed here.

The versatile reactions occurring in the Amyrel active site can be summarized as follows:

(i) Disproportionation with G_n as sole substrate and formation of the covalent glucosyl-enzyme intermediate EG1:

$$2 \ G_n \rightarrow G_{n-1} + G_{n+1}.$$

(ii) Hydrolysis of the covalent glucosyl-enzyme intermediate EG1:

$$G_n \rightarrow G_{n-1} + G1.$$

(iii) Disproportionation with other acceptors G_x, including G1:

$$G_n + G_x \rightarrow G_{n-1} + G_{x+1}.$$

(iv) Hydrolysis of the covalent glycosyl-enzyme intermediate EG_x, with G_y as a leaving group:

$$G_n \rightarrow G_x + G_y.$$

(v) Possible transglycosylation of the covalent glycosyl-enzyme intermediate EG_x with the acceptor G_z and with G_y as a leaving group:

$$G_n + G_z \rightarrow G_{x+z} + G_y \ (\text{with} \ x + y = n).$$

Some amino acid residues near the active site have been involved in the transglycosylase activity of microbial α-amylases (Rivera et al. 2003; Tran et al. 2014). However, these residues are not found in Amyrel, and their corresponding positions in the sequence are occupied by conserved residues in animal α-amylases, including

Amyrel. The availability of animal-type α-amylase crystal structures in complex with saccharides and substrate analogs allows identifying residues performing direct H-bonds with the substrate bound in the active site (Qian et al. 1994; Nahoum et al. 2000; Aghajari et al. 2002; Ramasubbu et al. 2003; Li et al. 2005). All these residues are conserved in Amyrel, with the noticeable exception of a His residue (His 305 in human and PPAs, at subsite −2) which is lacking in Amyrel. This His residue belongs to the so-called flexible loop, which is deleted in Amyrel. The deleted mutants Amy ΔGHGA and PPA ΔGHGA have convincingly demonstrated the key function of this deletion in the unusual reaction pattern of Amyrel as both mutants became able to disproportionate maltooligosaccharides and acquired a slight glucose-forming activity (Figure 6). It is also worth mentioning that a deletion engineered in the flexible loop of human salivary α-amylase also provided a glucose-forming activity but only on G3, G4 and G5 (Ramasubbu et al. 2003). In animal-type α-amylases in complex with substrate analogs, the large displacement of the flexible loop restricts access to the active site. It has been proposed that, in this conformation, the substrate might be tightly bound in its active site subsites but also that, when the loop returns to its initial position, it may promote product release (Qian et al. 1994; Aghajari et al. 2002; Ramasubbu et al. 2003). Since such a mobile loop is lacking in Amyrel, one can reasonably expect a higher degree of freedom for subsite occupancy by the substrate (as exemplified by G2–pNP, Figure 4) and to a less-constrained reaction pathway (such as hydrolysis only in α-amylases), leading to the versatile reactions occurring in the Amyrel active site. In animal α-amylases in complex with inhibitors, the His residue lacking in Amyrel performs direct H-bonding with substrate analogs at subsite −2: This aspect further supports a less-constrained binding mode of the substrate in Amyrel. It should be noted that deletion in the flexible loop is also observed in all Amyrel homologs from Diptera, in some other dipteran amylases and in some amylase gene copies of various insect orders. However, to the best of our knowledge, the reaction pattern of these enzymes has not been reported to date. The residue Trp142 in subsite +2 of all Amyrel homologs also participate to the peculiar mechanism as the mutation Tyr (conserved in α-amylases) to Trp provides a glucose-forming activity and G3 hydrolysis to the Amy mutant. A bulkier and more hydrophobic residue in positive subsites is expected to favor transglycosylation (Abdul Manas et al. 2018).

The physiological function of Amyrel in vivo remains elusive. Its low net hydrolytic activity (Table III) does not support a major involvement in starch digestion. One can therefore tentatively suggest that the synthesis of multiple maltooligosaccharides of various lengths by its 4-α-GTase activity could provide beneficial probiotic compounds to *Drosophila* or to the microbiota inhabiting the digestive tract of the fruit fly. It can possibly store glucose in the polymeric state of maltooligosaccharides, as suggested for an archaeal 4-α-GTase (Kaila and Guptasarma 2019). Amyrel could also participate in the metabolism of glycogen, as reported for microbial 4-α-GTases (van der Maarel and Leemhuis 2013). However, both latter functions are less likely because Amyrel is a secreted enzyme as demonstrated by the occurrence of a signal peptide in its sequence.

Materials and methods

Production and purification of proteins

The sequences of enzymes used in this study were the following: α-amylase Amy from *D. melanogaster* (GenBank BAB32511),

Amyrel from *D. melanogaster* (GenBank AAF57971) and PPA (GenBank NP_999360). Except for porcine pancreatic *α*-amylase (PPA) which was purchased from (Sigma, Saint Louis, MO) (A6255), the enzymes were produced in recombinant *Pichia pastoris* strains GS115 or KM71 (Invitrogen, Carlsbad, CA, USA) and were purified as described ([Commin et al. 2013](#); [Claisse et al. 2016](#)). Briefly, the recombinant enzymes were secreted in the supernatant as the major protein and were specifically precipitated using glycogen in alcoholic condition. After glycogen autodigestion and dialysis, the purified enzymes were checked for quality and were quantified by sodium dodecyl sulfate-polyacrylamide gel electrophoresis (SDS PAGE) ([Supplementary Figure S14](#)). The gene sequence for the PPA mutant PPA ΔGHGA, in which four consecutive residues were deleted, was synthetized by MWG (now Eurofins Genomics, Ebersberg, Germany) and the insert was transferred into the expression vector pPIC3.5 K (Invitrogen). The gene sequence for the *D. melanogaster* mutant Amy ΔGHGA was obtained by inverse polymerase chain reaction (PCR) from a pGEM-T plasmid containing the full-size Amy gene by using phosphorylated primers which were then transferred into the expression vector pPIC3.5 K.

Forward primer: GGTGCTGGAGGGGCTAGTATATTGAC-CTTTTGGGATG

Reverse primer: ATGACCTCTCTGATTATCGTGATTGTC-GACGAATAC

The mutants Amy Y142W and Amyrel W140Y were made by inverse PCR from pGEM-T clones containing the native full-size Amy and Amyrel genes, respectively, using the Q5 directed mutagenesis kit from NEB, then transferred into the expression vector pPIC3.5 K. The following primers were used for Amy Y142W:

Forward: GACGCCAACGAGGTGCGCAACTG

Reverse: GTTCCAGTTGCTGATGGCGCAGG

For Amyrel W140Y:

Forward: CGCTTCCAGGTGCAACAGTGC

Reverse: ATCGTTGTAGTCGGTAATCTC

Thin layer chromatography

Most substrates were purchased from Sigma: soluble starch (ref. 33615), maltotetraose to maltoheptaose (ref. 47872, 47873, 47876, 47877); maltotriose (M8378); *p*-nitrophenyl-maltoside (G2–*p*NP, N5885); *p*-nitrophenyl-glucoside (G1–*p*NP, N1377) and *p*-nitrophenol (ref. 1048). The G7–*p*NP (ref. 720 470) and Et–G7–*p*NP (also named EPS, 1492_977) were from (Boehringer, Mannheim, Germany); Et–G1 was purchased from (Carbosynth, Compton, UK). TLC was performed as described earlier ([Commin et al. 2013](#)). For ^{14}C labeling, maltotriose or maltotetraose (5 mg/mL) were mixed with 1% ^{14}C-glucose 400 μM prior to digestion by the enzyme. All digestions were performed at 37°C in 20 mM Hepes, 20 mM NaCl, 1 mM CaCl$_2$, pH 7.5.

Isothermal titration calorimetry

Activity and reaction time course were recorded by ITC and analyzed as described ([D'Amico et al. 2006](#); [Commin et al. 2013](#)) by using a MicroCal VP-ITC fitted with a 1.4-mL hastelloy cell and an injection syringe stirring at 310 rpm. Reactions were performed at 25°C in 20 mM Hepes, 20 mM NaCl, 1 mM CaCl$_2$, pH 7.5, with 1% soluble starch or 5 mM maltooligosaccharides as substrates.

MALDI-TOF-MS analysis

Mass determination of the synthesized maltooligosaccharides was performed on a MALDI-TOF-TOF (Matrix Assisted Laser Desorp-

tion Ionization – Time of Flight) mass spectrometer (MS) Rapiflex (Bruker Daltonics) in positive ion mode and in reflectron mode. External linear calibration in the mass range 160–3145 m/z was carried out using the Peptide Calibration Standard calibrant (Bruker). The standard deviation after calibration was <100 ppm. One μL of matrix was mixed with 1 μL of sample on plate.

Supplementary data

Supplementary data are available at *Glycobiology* online.

Data availability statement

The data underlying this article are available in the article and in its online supplementary data.

Acknowledgements

Funding

Conflict of interest statement

None declared.

Abbreviations

4-*α*-GTase, 4-*α*-glucanotransferase; DP, degree of polymerization; G$_n$, maltooligosaccharide with *n* glucopyrannose units; ITC, isothermal titration calorimetry; *p*NP, *p*-nitrophenyl group; PPA, porcine pancreatic *α*-amylase; TLC, thin layer chromatography.

References

Abdul Manas NH, Md Illias R, Mahadi NM. 2018. Strategy in manipulating transglycosylation activity of glycosyl hydrolase for oligosaccharide production. *Crit Rev Biotechnol*. 38(2):272–293.

Aghajari N, Roth M, Haser R. 2002. Crystallographic evidence of a transglycosylation reaction: Ternary complexes of a psychrophilic alpha-amylase. *Biochemistry*. 41(13):4273–4280.

Ahmad N, Mehboob S, Rashid N. 2015. Starch-processing enzymes—Emphasis on thermostable 4-*α*-glucanotransferases. *Biologia*. 70(6): 709–725.

Albenne C, Skov LK, Mirza O, Gajhede M, Potocki-Veronese G, Monsan P, Remaud-Simeon M. 2002. Maltooligosaccharide disproportionation reaction: An intrinsic property of amylosucrase from *Neisseria polysaccharea*. *FEBS Lett*. 527(1–3):67–70.

Andre G, Tran V. 2004. Putative implication of alpha-amylase loop 7 in the mechanism of substrate binding and reaction products release. *Biopolymers*. 75(2):95–108.

Bernfeld P. 1955. Amylases, alpha and beta. *Methods Enzymol*. 1:149–158.

Bijttebier A, Goesaert H, Delcour JA. 2008. Amylase action pattern on starch polymers. *Biologia*. 63(6):989–999.

Claisse G, Feller G, Bonneau M, Da Lage JL. 2016. A single amino-acid substitution toggles chloride dependence of the alpha-amylase paralog amyrel in *Drosophila melanogaster* and *Drosophila virilis* species. *Insect Biochem Mol Biol*. 75:70–77.

Clowers BH, Dodds ED, Seipert RR, Lebrilla CB. 2008. Dual polarity accurate mass calibration for electrospray ionization and matrix-assisted laser desorption/ionization mass spectrometry using maltooligosaccharides. *Anal Biochem*. 381(2):205–213.

Commin C, Aumont-Nicaise M, Claisse G, Feller G, Da Lage JL. 2013. Enzymatic characterization of recombinant alpha-amylase in the *Drosophila melanogaster* species subgroup: Is there an effect of specialization on digestive enzyme? *Genes Genet Syst*. 88(4):251–259.

D'Amico S, Gerday C, Feller G. 2000. Structural similarities and evolutionary relationships in chloride-dependent alpha-amylases. *Gene*. 253(1):95–105.

D'Amico S, Sohier JS, Feller G. 2006. Kinetics and energetics of ligand binding determined by microcalorimetry: Insights into active site mobility in a psychrophilic alpha-amylase. *J Mol Biol*. 358(5):1296–1304.

Da Lage JL, Binder M, Hua-Van A, Janecek S, Casane D. 2013. Gene make-up: Rapid and massive intron gains after horizontal transfer of a bacterial alpha-amylase gene to basidiomycetes. *BMC Evol Biol*. 13(1):40.

Da Lage JL, Danchin EG, Casane D. 2007. Where do animal alpha-amylases come from? An interkingdom trip. *FEBS Lett*. 581(21):3927–3935.

Da Lage JL, Renard E, Chartois F, Lemeunier F, Cariou ML. 1998. *Amyrel*, a paralogous gene of the amylase gene family in *Drosophila melanogaster* and the *Sophophora* subgenus. *Proc Natl Acad Sci U S A*. 95(12):6848–6853.

Da Lage JL, van Wormhoudt A, Cariou ML. 2002. Diversity and evolution of the alpha-amylase genes in animals. *Biologia*. 57:181–189.

Kaila P, Guptasarma P. 2019. An ultra-stable glucanotransferase-cum-exoamylase from the hyperthermophile archaeon *Thermococcus onnurineus*. *Arch Biochem Biophys*. 665:114–121.

Kaila P, Mehta GS, Dhaunta N, Guptasarma P. 2019. Structure-guided mutational evidence and postulates explaining how a glycohydrolase from *Pyrococcus furiosus* functions simultaneously as an amylase and as a 4-alpha-glucanotransferase. *Biochem Biophys Res Commun*. 509(4):892–897.

Li C, Begum A, Numao S, Park KH, Withers SG, Brayer GD. 2005. Acarbose rearrangement mechanism implied by the kinetic and structural analysis of human pancreatic alpha-amylase in complex with analogues and their elongated counterparts. *Biochemistry*. 44(9):3347–3357.

Lombard V, Golaconda Ramulu H, Drula E, Coutinho PM, Henrissat B. 2014. The carbohydrate-active enzymes database (CAZy) in 2013. *Nucleic Acids Res*. 42(D1):D490–D495.

Maczkowiak F, Da Lage JL. 2006. Origin and evolution of the *Amyrel* gene in the alpha-amylase multigene family of Diptera. *Genetica*. 128 (1–3):145–158.

Mazur AK, Nakatani H. 1993. Multiple attack mechanism in the porcine pancreatic alpha-amylase hydrolysis of amylose and amylopectin. *Arch Biochem Biophys*. 306(1):29–38.

Nahoum V, Roux G, Anton V, Rouge P, Puigserver A, Bischoff H, Henrissat B, Payan F. 2000. Crystal structures of human pancreatic alpha-amylase in complex with carbohydrate and proteinaceous inhibitors. *Biochem J*. 346(1):201–208.

Pan S, Ding N, Ren J, Gu Z, Li C, Hong Y, Cheng L, Holler TP, Li Z. 2017. Maltooligosaccharide-forming amylase: Characteristics, preparation, and application. *Biotechnol Adv*. 35(5):619–632.

Qian M, Haser R, Buisson G, Duee E, Payan F. 1994. The active center of a mammalian alpha-amylase. Structure of the complex of a pancreatic alpha-amylase with a carbohydrate inhibitor refined to 2.2-Å resolution. *Biochemistry*. 33(20):6284–6294.

Ramasubbu N, Ragunath C, Mishra PJ. 2003. Probing the role of a mobile loop in substrate binding and enzyme activity of human salivary amylase. *J Mol Biol*. 325(5):1061–1076.

Remenyik J, Ragunath C, Ramasubbu N, Gyemant G, Liptak A, Kandra L. 2003. Introducing transglycosylation activity into human salivary alpha-amylase (HSA). *Org Lett*. 5(25):4895–4898.

Rivera MH, Lopez-Munguia A, Soberon X, Saab-Rincon G. 2003. Alpha-amylase from *Bacillus licheniformis* mutants near to the catalytic site: Effects on hydrolytic and transglycosylation activity. *Protein Eng*. 16(7):505–514.

Robyt JF, French D. 1970. The action pattern of porcine pancreatic alpha-amylase in relationship to the substrate binding site of the enzyme. *J Biol Chem*. 245(15):3917–3927.

Stam MR, Danchin EG, Rancurel C, Coutinho PM, Henrissat B. 2006. Dividing the large glycoside hydrolase family 13 into subfamilies: Towards improved functional annotations of alpha-amylase-related proteins. *Protein Eng Des Sel*. 19(12):555–562.

Takaha T, Smith SM. 1999. The functions of 4-alpha-glucanotransferases and their use for the production of cyclic glucans. *Biotechnol Genet Eng Rev*. 16(1):257–280.

Tran PL, Cha HJ, Lee JS, Park SH, Woo EJ, Park KH. 2014. Introducing transglycosylation activity in *Bacillus licheniformis* alpha-amylase by replacement of His235 with Glu. *Biochem Biophys Res Commun*. 451(4):541–547.

Uitdehaag JC, Mosi R, Kalk KH, van der Veen BA, Dijkhuizen L, Withers SG, Dijkstra BW. 1999. X-ray structures along the reaction pathway of cyclodextrin glycosyltransferase elucidate catalysis in the alpha-amylase family. *Nat Struct Biol*. 6(5):432–436.

van der Maarel MJ, Leemhuis H. 2013. Starch modification with microbial alpha-glucanotransferase enzymes. *Carbohydr Polym*. 93(1): 116–121.

Xu Q, Cao Y, Li X, Liu L, Qin S, Wang Y, Cao Y, Xu H, Qiao D. 2018. Purification and characterization of a novel intracellular alpha-amylase with a wide variety of substrates hydrolysis and transglycosylation activity from *Paenibacillus* sp. SSG-1. *Protein Expr Purif*. 144: 62–70.

Zhai L, Feng L, Xia L, Yin H, Xiang S. 2016. Crystal structure of glycogen debranching enzyme and insights into its catalysis and disease-causing mutations. *Nat Commun*. 7(1):11229.